J|A|C|S
ARTICLES
Published on Web 09/12/2006

The Catalytic Mechanism of Peptidylglycine α-Hydroxylating Monooxygenase Investigated by Computer Simulation

Alejandro Crespo,[†,‡] Marcelo A. Martí,[†] Adrian E. Roitberg,[‡] L. Mario Amzel,*[,§] and Darío A. Estrin*[,†]

Contribution from the Departamento de Química Inorgánica, Analítica y Química-Física and INQUIMAE-CONICET, Facultad de Ciencias Exactas y Naturales, Universidad de Buenos Aires, Ciudad Universitaria, Pab. 2, C1428EHA Buenos Aires, Argentina, Quantum Theory Project and Department of Chemistry, University of Florida, Gainesville, Florida 32611-8435, and Department of Biophysics and Biophysical Chemistry, Johns Hopkins School of Medicine, Johns Hopkins University, Baltimore, Maryland 21205

Received April 25, 2006; E-mail: mario@neruda.med.jhmi.edu; dario@qi.fcen.uba.ar

Abstract: The molecular basis of the hydroxylation reaction of the Cα of a C-terminal glycine catalyzed by peptidylglycine α-hydroxylating monooxygenase (PHM) was investigated using hybrid quantum-classical (QM-MM) computational techniques. We have identified the most reactive oxygenated species and presented new insights into the hydrogen abstraction (H-abstraction) mechanism operative in PHM. Our results suggest that O_2 binds to Cu_B to generate $Cu_B^{II}-O_2^{\bullet -}$ followed by electron transfer (ET) from Cu_A to form $Cu_B^{I}-O_2^{\bullet -}$. The computed potential energy profiles for the H-abstraction reaction for $Cu_B^{II}-O_2^{\bullet -}$, $Cu_B^{I}-O_2^{\bullet -}$, and $[Cu_B^{II}-OOH]^+$ species indicate that none of these species can be responsible for abstraction. However, the latter species can spontaneously form $[Cu_BO]^{+2}$ (which consists of a two-unpaired-electrons $[Cu_BO]^+$ moiety ferromagneticaly coupled with a radical cation located over the three Cu_B ligands, in the quartet spin ground state) by abstracting a proton from the surrounding solvent. Both this monooxygenated species and the one obtained by reduction with ascorbate, $[Cu_BO]^+$, were found to be capable of carrying out the H-abstraction; however, whereas the former abstracts the hydrogen atom concertedly with almost no activation energy, the later forms an intermediate that continues the reaction by a rebinding step. We propose that the active species in H-abstraction in PHM is probably $[Cu_BO]^{+2}$ because it is formed exothermically and can concertedly abstract the substrate HA atom with the lower overall activation energy. Interestingly, this species resembles the active oxidant in cytochrome P450 enzymes, Compound I, suggesting that both PHM and cytochrome P450 enzymes may carry out substrate hydroxylation by using a similar mechanism.

Introduction

Copper proteins are common in biology and play important roles in O_2 activation and reduction.[1−3] One such enzyme, peptidylglycine α-amidating monooxygenase (PAM) is responsible for the activation of many peptide hormones and neuropeptides that require amidation of their C terminus for biological activity.[4−6] PAM uses separate enzymatic domains to catalyze this amidation reaction in two steps: (i) hydroxylation of the Cα of a C-terminal glycine and (ii) disproportionation of the α-hydroxyglycine.[7,8] The first step is catalyzed by the peptidylglycine α-hydroxylating monooxygenase (PHM), a two-copper, ascorbate-dependent enzyme that is the more extensively studied of the two PAM domains (see Scheme 1). Kinetic and mutagenesis studies,[9,10] detailed kinetic isotope effect measurements,[11−14] and extended X-ray absorption fine structure measurements,[10,15−17] as well as determination of the structures of several forms of the enzyme,[18,19] have been used

† Universidad de Buenos Aires.
‡ University of Florida.
§ Johns Hopkins University.

(1) Holm, R. H.; Kennepohl, P.; Solomon, E. I. *Chem. Rev.* **1996**, *96*, 2239−2314.
(2) Solomon, E. I.; Sundaram, U. M.; Machonkin, T. E. *Chem. Rev.* **1996**, *96*, 2563−2606.
(3) Klinman, J. P. *Chem. Rev.* **1996**, *96*, 2541−2562.
(4) Cuttitta, F. *Anat. Rec.* **1993**, *236*, 87−93.
(5) Merkler, D. J. *Enzyme Microb. Technol.* **1994**, *16*, 450−456.
(6) Eipper, B. A.; Stoffers, D. A.; Mains, R. E. *Annu. Rev. Neurosci.* **1992**, *15*, 57−85.
(7) Bradbury, A. F.; Finnie, M. D.; Smyth, D. G. *Nature* **1992**, *298*, 686−688.
(8) Eipper, B. A.; Milgram, S. L.; Husten, E. J.; Yun, H. Y.; Mains, R. E. *Protein Sci.* **1993**, *2*, 489−97.
(9) Bell, J.; El Meskini, R.; D'Amato, D.; Mains, R. E.; Eipper, B. A. *Biochemistry* **2003**, *42*, 7133−7142.
(10) Eipper, B. A.; Quon, A. S.; Mains, R. E.; Boswell, J. S.; Blackburn, N. J. *Biochemistry* **1995**, *34*, 2857−2865.
(11) Takahashi, K.; Onami, T.; Noguchi, M. *Biochem. J.* **1998**, *336*, 131−137.
(12) Francisco, W. A.; Merkler, D. J.; Blackburn, N. J.; Klinman, J. P. *Biochemistry* **1998**, *37*, 824 4−8252.
(13) Francisco, W. A.; Knapp, M. J.; Blackburn, N. J.; Klinman, J. P. *J. Am. Chem. Soc.* **2002**, *124*, 8194−8195.
(14) Francisco, W. A.; Blackburn, N. J.; Klinman, J. P. *Biochemistry* **2003**, *42*, 1813−1819.
(15) Blackburn, N. J.; Rhames, F. C.; Ralle, M.; Jaron, S. *J. Biol. Inorg. Chem.* **2000**, *5*, 341−353.
(16) Boswell, J. S.; Reedy, B. J.; Kulathila, R.; Merkler, D.; Blackburn, N. J. *Biochemistry* **1996**, *35*, 12241−12250.
(17) Jaron, S.; Blackburn, N. J. *Biochemistry* **2001**, *40*, 6867−6875.
(18) Prigge, S. T.; Kolhekar, A. S.; Eipper, B. A.; Mains, R. E.; Amzel, L. M. *Science* **1997**, *278*, 1300−1306.

Scheme 1. Stoichiometry of the Global Reaction Catalyzed by PHM

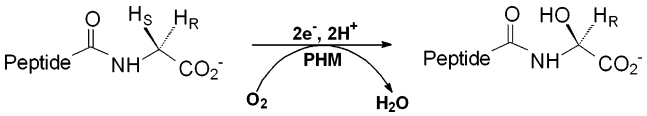

to understand the reaction carried out by PHM. Despite these intense efforts, key aspects of the PHM mechanism remain elusive.[9,20,21] Perhaps the most puzzling aspects of the PHM reaction are the mechanism of electron transfer between the active-site coppers, the subsequent reduction of molecular oxygen, and hydrogen abstraction (H-abstraction). Crystallographic, spectroscopic, and kinetic studies have provided conflicting information about how electrons are transferred between the copper atoms and how the chemical steps of the PHM reaction take place. Depending on the coordination of the dioxygen to Cu, the copper-bound oxygen may also be a part of the electron-transfer path, coupling electron transfer to oxygen reduction and H-abstraction.

Another well-characterized enzyme related to PHM is dopamine β-monooxygenase (DβM), which catalyzes the hydroxylation of the dopamine benzylic Cβ using molecular O_2 in a stereo- and regiospecific fashion in the same way as PHM does.[3] The active sites of DβM and PHM both consist of two inequivalent Cu centers (Cu_H or Cu_A and Cu_M or Cu_B) widely separated in space (~11 Å in PHM)[18] with no direct bridging ligands and no observable magnetic interactions.[22] The crystal structure of PHM indicates that at the Cu_B site (where dioxygen coordinates and substrate hydroxylation occurs) Cu is coordinated by two histidine and one methionine ligands and at the Cu_A site (which provides an additional electron through long-range electron transfer (ET) to the Cu_B site) Cu is coordinated to three histidine ligands from the protein.[3,18,19] Since the two Cu sites in PHM and DβM are far apart, the mechanism for this long-range ET is not clear. Two mechanisms have been proposed to account for this inter-copper intramolecular ET process: a superoxide channeling mechanism[20] and a substrate-facilitated ET mechanism (through the substrate[19] or protein residues brought closer upon substrate binding[9]).

Previous kinetic and mechanistic studies have shown that the reaction mechanisms for substrate hydroxylation in PHM and DβM are very similar.[3] The enzymatic cycle starts with both the Cu_A and Cu_B sites in the Cu^I oxidation state (reduced by ascorbate under physiological conditions). When a substrate is present, O_2 reacts with the reduced protein, forming a reactive Cu/O_2 intermediate, which then cleaves the substrate C−H bond via an H-atom abstraction mechanism, generating a substrate radical (the abstracted H-atom is the *pro-S* HA, and the one left is the *pro-R* HA, see Scheme 1).[23−26] Significant ^2H and ^{18}O isotope effects have been observed on the C−H bond cleavage reaction leading to the final hydroxylated

Scheme 2. Possible Reaction Pathways Studied by Chen and Solomon[28]

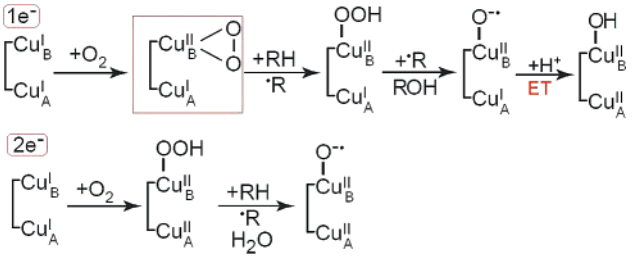

product.[3,12−14,25,27] The reactive Cu/O_2 intermediate has been widely proposed to be an as-yet unobserved $[Cu^{II}-OOH]^+$ species that would either abstract the substrate hydrogen directly or after forming a Cu^{II}−oxyl intermediate.[3] A $Cu^{II}-O_2^{2-}/Cu^I-O_2^{\bullet-}$ species has also been proposed by Prigge as a possible reactive intermediate for the H-atom abstraction reaction.[21]

Chen and Solomon[28] studied the oxygen activation and the reaction mechanism of PHM in model systems by using DFT methods. They calculated the reaction thermodynamics and potential energy surfaces of two possible reactive Cu/O_2 species: the one-electron reduced $[Cu^{II}-OOH]^+$ (Scheme 2, bottom) and the one-electron reduced side-on Cu^{II}−superoxo (Scheme 2, top) intermediates. The authors found that the substrate H-atom abstraction by $[Cu^{II}-OOH]^+$ was thermodynamically feasible but has a very high activation barrier (37 kcal/mol). In contrast, H-atom abstraction from the substrate by the second intermediate was found to be nearly isoenergetic, with a low reaction barrier (14 kcal/mol), suggesting that this is the reactive species. They also proposed a pathway for a subsequent substrate hydroxylation involving a "water-assisted" direct OH transfer to the substrate radical, generating a high-energy Cu^{II}−oxyl species that would provide the driving force that allows completion of the ET. Moreover, Decker and Solomon[29] have recently reported a comparative study of dioxygen activation by copper, heme, and non-heme iron enzymes. They concluded, on the basis of the ligand environment and the redox properties of the metal, that these enzymes employ different methods of dioxygen activation. Heme enzymes are able to stabilize the very reactive iron(IV)−oxo porphyrin-radical intermediate as in cytochrome P450 enzymes. This is generally not accessible for non-heme iron systems, which can instead use low-spin ferric−hydroperoxo and iron(IV)−oxo species as reactive oxidants. Finally, they suggest that copper enzymes employ a different strategy and achieve H-atom abstraction potentially through a superoxo intermediate.[28] However, we will show that both PHM and cytochrome P450 enzymes may carry out substrate hydroxylation by using a similar mechanism.

Kamachi et al.[30] investigated the dopamine hydroxylation by copper−superoxo, −hydroperoxo, and −oxo species in DβM to identify the active species in the reaction and reveal the key functions of the surrounding amino acid residues in substrate binding (see Scheme 3). The authors carried out DFT/QM-MM optimizations followed by evaluation of the reactivity of the three oxidants by QM using small model systems extracted from

(19) Prigge, S. T.; Kolhekar, A. S.; Eipper, B. A.; Mains, R. E.; Amzel, L. M. *Nature Struct. Biol.* **1999**, *6*, 976−983.
(20) Jaron, S.; Blackburn, N. J. *Biochemistry* **1999**, *38*, 15086−15096.
(21) Prigge, S. T.; Mains, R. E.; Eipper, B. A.; Amzel, L. M. *Cell. Mol. Life Sci.* **2000**, *57*, 1236−1259.
(22) Ljones, T.; Skotland, T. In *Copper Proteins and Copper Enzymes*; Lontie, R.; Ed.; CRC Press: Boca Raton, FL, **1984**; Vol. 2, p 131−157.
(23) Fitzpatrick, P. F.; Flory, D. R.; Villafranca, J. J. *Biochemistry* **1985**, *24*, 2108−2114.
(24) Fitzpatrick, P. F.; Villafranca, J. J. *J. Am. Chem. Soc.* **1985**, *107*, 5022−5023.
(25) Miller, S. M.; Klinman, J. P. *Biochemistry* **1985**, *24*, 2114−2127.
(26) Wimalasena, K.; May, S. W. *J. Am. Chem. Soc.* **1989**, *111*, 2729−2731.
(27) Stewart, L. C.; Klinman, J. P. *Annu. Rev. Biochem.* **1988**, *57*, 551−592.
(28) Chen, P.; Solomon, E. I. *J. Am. Chem. Soc.* **2004**, *126*, 4991−5000.
(29) Decker, A.; Solomon, E. I. *Curr. Op. Chem. Biol.* **2005**, *9*, 152−163.
(30) Kamachi, T.; Kihara, N.; Shiota, Y.; Yoshizawa, K. *Inorg. Chem.* **2005**, *44*, 4226−4263.

Scheme 3. Reaction Mechanism Studied by Kamachi et al.[30] and Proposed Active Species Responsible for H-Abstraction

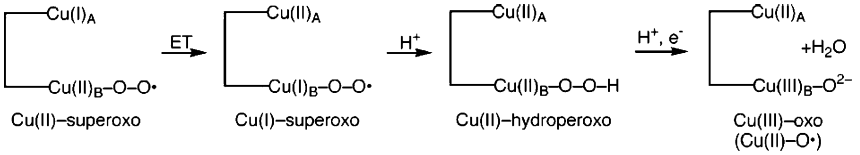

the QM-MM simulations of the whole-enzyme model, obtained by homology modeling using the crystal structure of PHM. The activation energies for the H-abstraction from the substrate by the Cu^{II}−superoxo moiety and the subsequent O−O cleavage and OH group transfer to the substrate radical were found to be ∼17 kcal/mol and ∼10 kcal/mol respectively, suggesting that the Cu^{II}−superoxo species can promote the H-abstraction in DβM. The Cu^{II}−hydroperoxo species was ruled out as an active oxidant, because the activation barrier of that H-abstraction was found to be more than 40 kcal/mol. Finally, they concluded that the Cu^{III}−oxo species reasonably promotes the H-abstraction because the activation energy was found to be only 3.8 kcal/mol, and 6.5 kcal/mol for the final rebinding step. More recently, these authors performed calculations for a full enzyme QM-MM model and obtained similar results.[31]

Tian et al.[32] proposed an oxo-mediated radical mechanism that is consistent with the results of the kinetic isotope effects studies, where the O−O bond breaks before the C−H bond. In their mechanism the Cu^{II}−hydroperoxo species abstracts a hydrogen atom from a nearby tyrosine residue to produce a Cu^{III}−oxo species, a tyrosyl radical, and a water molecule. The Cu^{III}−oxo species abstracts a hydrogen atom from the benzylic position of dopamine with formation of a radical intermediate. However, recent mutational studies[14] demonstrated that the catalytic activity of a Y318F mutant of PHM remains unchanged from the wild-type enzyme, implying that the Tyr318 residue in PHM is not essential.

The Cu^{II}−superoxo species, produced by dioxygen binding to the Cu_B center in the resting Cu^I state, was proposed by Evans et al.[33] to be responsible for the C−H bond activation in DβM. This mechanism involves an initial hydrogen-atom abstraction from the benzylic position of dopamine, followed by recombination between the substrate radical and the resultant Cu^{II}−hydroperoxo species to form norepinephrine. In this mechanism electron transfer from the Cu_A center occurs after the C−H bond activation. They also demonstrated[33] that a molar ratio of O_2 consumption to product formation is 1:1 not only for highly reactive substrates but also for weakly reactive substrates. A mechanism in which reductive activation of dioxygen precedes the C−H bond cleavage cannot explain such a tight coupling of oxygen and substrate consumption because either peroxide or superoxide leaks into the solvent from the reactive oxygen intermediate with extended lifetime.

Recently, Prigge et al.[34] solved the X-ray structure of the precatalytic complex of PHM with bound peptide and oxygen, at 1.85 Å resolution. This work provided insight into several geometric and mechanistic characteristics of the PHM catalytic mechanism. First, in the precatalytic complex, dioxygen binds to the highly solvent-exposed Cu_B site with an end-on η^1 geometry. The Cu_B−O−O angle is 110°, and the O−O distance refined to a value of 1.23 Å. This geometry is compatible with either dioxygen or superoxide bound to copper, but not with Cu−peroxo species. They also proposed that an ET pathway between Cu_A and Cu_B is possible only when peptide substrate binds to reduced PHM,[19] and this pathway linked His_{108} (a Cu_A ligand), a water molecule, and the C terminus of the substrate through hydrogen bonds allowing ET from Cu_A to the Cu_B−dioxygen species (Cu_B^{II}−$O_2^{\bullet-}$). The resulting reduced oxygen species (Cu_B^{I}−$O_2^{\bullet-}$) abstracts the glycine *pro-S* hydrogen of the peptide substrate (Scheme 4). H-abstraction requires that one of the oxygen atoms of O_2 comes in contact with the glycine *pro-S* hydrogen. A rotation of the distal oxygen atom by ∼110° around the Cu_B−O bond places the distal oxygen atom about 2.2 Å from the hydrogen atom—an ideal position to facilitate the H-abstraction step. Inspection of the structure indicates that the barrier for this rotation is probably small and that thermal rotation of the distal oxygen atom could place it at a short distance from the glycine *pro-S* hydrogen. Because the Cu−O_2 complex was not observed in structures of oxidized PHM or in structures of reduced PHM without substrate, the authors propose that the substrate binds to the reduced enzyme before oxygen can bind, which prevents binding and activation of oxygen unless catalysis is primed to proceed.

Klinman[35] reviewed previous work on the H-abstraction reaction catalyzed for both PHM and DβM, pointing out that both enzymes are mechanistically interchangeable and that hydrogen transfer is not classical. Four possible mechanisms for O_2 activation in DβM and PHM were proposed in that work, ranging from the formation of a one-electron reduced intermediate (metal superoxo, Cu^{II}−$O_2^{\bullet-}$), Mechanism I, to two-electron reduced species (metal peroxo, Cu^{II}−O_2^{2-}), Mechanism II, or metal hydroperoxo ([Cu^{II}−OOH]$^+$), Mechanism III, and finally to a highly reduced Cu^{III}−oxo species formed via the reductive cleavage of [Cu^{II}−OOH]$^+$ by a conserved active-site tyrosine, Mechanism IV. The site-specific mutagenesis experiments mentioned before,[14] however, effectively eliminated Mechanism IV from consideration. Moreover, the large driving force for formation of H_2O_2 from O_2 suggested that the [Cu^{II}−OOH]$^+$ (Mechanism III) may not be a good candidate for the activated O_2 species in DβM and PHM, which was later verified experimentally.[33] In addition to eliminating a metal hydroperoxide from consideration, the available data also appear to rule out a mechanism in which O_2 was proposed to bind initially to Cu_A to form a Cu_A^{II}−$O_2^{\bullet-}$ intermediate, followed by dissociation of the superoxide anion and its migration across the solvent interface to bind and be further reduced at Cu_B.[20] Furthermore, mechanism II, involving the Cu(II)−peroxy anion as the oxygenating species was also eliminated, because the X-ray geometry is not compatible with a copper−peroxo species.[34] Finally, the author concluded that Mechanism I, the formation

(31) Yoshizawa, K.; Kihara, N.; Kamachi, T.; Shiota, Y. *Inorg. Chem.* **2006**, *45*, 3034−3041.
(32) Tian, G.; Berry, J. A.; Klinman, J. P. *Biochemistry* **1994**, *33*, 226−234.
(33) Evans, J. P.; Ahn, K.; Klinman, J. P. *J. Biol. Chem.* **2003**, *278*, 49691−49698.
(34) Prigge, S. T.; Eipper, B. A.; Mains, R. E.; Amzel, L. M. *Science* **2004**, *304*, 864−867.
(35) Klinman, J. P. *J. Biol. Chem.* **2006**, *281*, 3013−3016.

Scheme 4. Reaction Mechanism Proposed by Prigge et al.[34]

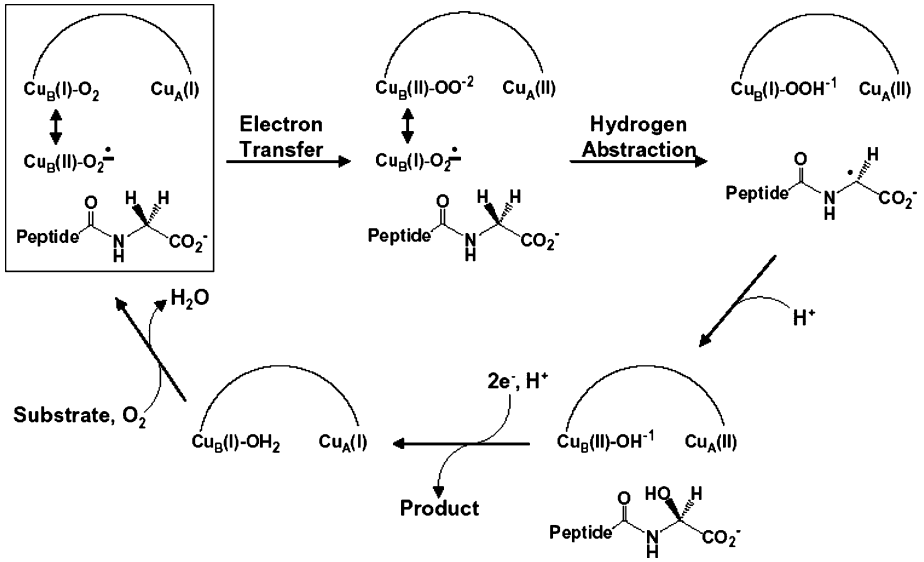

Scheme 5. Copper Superoxo Mechanism Proposed by Klinman[35]

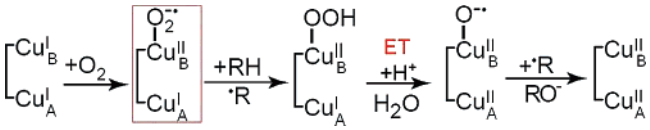

of a copper−superoxo intermediate, appears to provide a working mechanism that is capable of rationalizing the voluminous amount of data available for DβM and PHM, proposing the copper−superoxo as the active oxygen species (Scheme 5) and providing an answer to the long-standing question of how these enzymes catalyze electron transfer across bulk water at a rate that is compatible with catalytic turnover.

Finally, it is interesting to remark that dioxygen binding at the Cu_B site is now well supported by the existing literature, particularly by the fact that, in the recent published X-ray structure of the precatalytic complex of PHM with bound peptide and dioxygen, it binds to the highly solvent-exposed Cu_B site with an end-on η^1 geometry.[34] In most theoretical[28−31] and experimental[32,33,35] works, O_2 is assumed to be coordinated to Cu_B. However, it is clear that there is no consensus on the mechanism of the PHM reaction and/or the identity of the active species responsible for H-abstraction. In this work we investigated the molecular basis of the H-abstraction mechanism in PHM using QM-MM calculations. We calculated the O_2 binding energy to the Cu_B site in both oxidation states, before and after ET, as well as in presence and absence of the substrate. We also computed the rotational barrier of the distal oxygen atom around the Cu_B−O bond to assess the role of this motion in the catalytic mechanism. Finally, we identified the most reactive oxygenated species, characterized its formation, and investigated the H-abstraction mechanism operating in PHM. We propose that the active species is probably $[L_3^{\bullet+}Cu_B^{III}O]^{+2}$, which consists of a two-unpaired-electrons $[Cu_BO]^+$ moiety ferromagneticaly coupled with a radical cation located over the three Cu_B ligands in the quartet spin ground state, and suggest that both PHM and cytochrome P450 enzymes may carry out substrate hydroxylation by using a similar mechanism. The conclusions of this study may apply to other copper−oxygen-activating enzymes, such as DβM, and to the design of biomimetic complexes.

Methods

Simulations were performed starting from the crystal structure of PHM with bound peptide and coordinated dioxygen, at 1.85 Å resolution (PDB entry 1sdw).[34] Hydrogen atoms were added favoring H-bonding, and the system was solvated using a 40 Å water cap. Three Na^+ atoms were added to neutralize the system. The final system contains the model protein, 6217 water molecules, and the added ions, leading to a total of 23478 atoms. The classical optimized system was then heated and equilibrated in three steps: (i) 20 ps of MD heating the whole system from 100 to 200 K, (ii) heating of the entire system from 200 to 298 K for 20 ps, and (iii) equilibration of the entire system for 50 ps at 298 K.

The resulting structure was further equilibrated by performing a 1 ns classical MD simulations at 298 K to obtain correct QM-MM starting geometries. All classical simulations were performed using the Amber8 package.[36] Amber99[37] and TIP3P force fields were used to describe the protein/substrate and water, respectively. SHAKE was used to keep bonds involving H atoms at their equilibrium length.[38] For nonbonded interactions a 12 Å cutoff was employed. The simulations were performed using the Berendsen thermostat,[39] with a time step of 1 fs.

Both Cu_A and Cu_B model system charges were determined using RESP[40] charges and HF/6-31G(d) wave functions following the protocol recommended in the Amber web page.[41] The van der Waals parameters were taken from Amber99.[37] Even though the presence of transition metals introduces additional challenges, MD simulations are now commonly used for the investigation of metalloproteins.[42] Cu_B was coordinated to the side chains of residues Met_{314}, His_{242}, and His_{244} and to the bound oxygen in a tetrahedral geometry and Cu_A to side chains of residues His_{107}, His_{108}, and His_{172} also in a tetrahedral manner, as reported in the X-ray structure.[34] The equilibrium parameters were taken from the X-ray structure, and the S_{Met314}−Cu−O1−O2 dihedral angle was fixed at its crystallographic value of 40° during all simulations

(36) Cornell, W. D.; Cieplak, P.; Bayly, C. I.; Gould, I. R.; Merz, K. M., Jr.; Ferguson, D. M.; Spellmeyer, D. C.; Fox, T.; Caldwell, J. W.; Kollman, P. A. *J. Am. Chem. Soc.* **1995**, *117*, 5179−5197.
(37) Wang, J.; Cieplak, P.; Kollman, P. A. *J. Comput. Chem.* **2000**, *21*, 1049−1074.
(38) Ryckaert, J. P.; Ciccotti, G.; Berendsen, H. J. C. *J. Comput. Phys.* **1977**, *23*, 327−341.
(39) Berendsen, H. J. C.; Postma, J. P. M.; van Gunsteren, W. F.; Di Nola, A.; Haak, J. R. *J. Chem. Phys.* **1984**, *81*, 3684−3690.
(40) Bayly, C. I.; Cieplak, P.; Cornell, W. D.; Kollman, P. A. *J. Phys. Chem.* **1993**, *97*, 10269−10280.
(41) www.amber.scripts.edu
(42) Banci, L. *Curr. Op. Chem. Biol.* **2003**, *7*, 143−149.

Table 1. High-Spin/Low-Spin Energy Gaps (kcal/mol), Mulliken Charges and Spin Populations (in parenthesis) (*e*) and Oxygen Binding Energies (ΔE_L, kcal/mol), for Systems with and without Coordinated Substrate before and after ET

	$Cu_B^{II}–O^{\bullet-}$				$Cu_B^{I}–O_2^{\bullet-}$			
	with substrate		without substrate		with substrate		without substrate	
	oxy	free	oxy	free	oxy	free	oxy	free
ground spin state	triplet	singlet	triplet	singlet	doublet	doublet	doublet	doublet
ΔE_{HS-LS}	−4.4	67.5	−4.4	63.2	79.5	53.6	30.0	70.3
Cu	0.562	0.322	0.534	0.342	0.537	0.038	0.533	0.320
	(0.416)	(0.0)	(0.398)	(0.0)	(0.189)	(0.578)	(0.199)	(0.022)
O1	−0.200	−	−0.175	−	−0.426	−	−0.435	−
	(0.692)		(0.719)		(0.348)		(0.339)	
O2	−0.204	−	−0.214	−	−0.459	−	−0.508	−
	(0.724)		(0.730)		(0.431)		(0.434)	
ΔE_L	−19.5		−21.7		−68.8		−52.8	

in order to start our QM-MM calculations from that value (see Supporting Information for further details).

QM-MM calculations[43−48] were carried out to explore the effect of the environment on O_2 binding and rotational energy and in the H-abstraction reaction. We employed our own QM-MM implementation[49] in which the QM subsystem is treated at the DFT level using the program SIESTA.[50] The use of standard norm-conserving pseudopotentials[51] avoids the computation of core electrons, smoothing the valence charge density at the same time. In the present study, the nonlinear partial-core correction[52] is applied to the Cu atom. For all atoms, basis sets of double-ζ plus polarization quality were employed, with a pseudoatomic orbital energy shift of 30 meV and a grid cutoff of 150 Ry.[50] Calculations were performed using the generalized gradient approximation functional proposed by Perdew, Burke, and Ernzerhof.[53] This combination of functional, basis sets, and grid parameters has been validated for both Cu_A and Cu_B isolated model systems. The classical subsystem was treated using the Amber99 force field parametrization.[37] (See Supporting Information for Cu basis set and pseudopotential.)

The initial structure for QM-MM calculations was taken from the last nanosecond of the classical MD simulation. During this nanosecond of classical MD simulation, the root-mean-square deviation (rmsd, See Supporting Information) of the protein backbone was lower than 1.3 Å, compared to the X-ray structure, whose resolution is 1.85 Å, concluding that the resulting system was in fact stable and that the structure obtained to start the QM-MM calculations does not differ significantly from the X-ray structure. Cu_B plus the coordinated side chains of residues His_{242}, His_{244}, and Met_{314} and the O_2 ligand and a formyl glycine substrate were selected as the quantum subsystem, which comprises 41 atoms. The rest of the protein, including the Cu_A center, and the water molecules were treated classically (23441 atoms). We allowed free motion for QM atoms and for the MM atoms located inside a sphere of 13.5 Å from the QM subsystem center of mass. The frontier between the QM and MM portions of the system was treated by the SPLAM method.[54]

Ligand affinities (ΔE_L) were calculated using eq 1, where E_{Enz-L} is the energy of the ligand-bound enzyme, E_{Enz} is the energy of the ligand free enzyme, and E_L is the energy of the isolated ligand:

$$\Delta E_L = E_{Enz-L} - E_L - E_{Enz} \quad (1)$$

Obtaining accurate free energy profiles requires extensive sampling, which is computationally very expensive and difficult to achieve at the DFT QM-MM level. For these reasons potential energy profiles were determined using restrained energy minimizations along the reaction path that connects reactant and product states.[49] For this purpose, an additional term was added to the potential energy according to $V(\xi) = k(\xi - \xi_0)^2$, where k is an adjustable force constant, ξ is the value of the reaction coordinate in the system-particular configuration, and ξ_0 is the reference value of the reaction coordinate (see below for the choice of the reaction coordinate in the different cases). By varying ξ_0, the system is forced to follow the minimum reaction path along the given coordinate. The force constant for reaction coordinates involving distances was 200 kcal/(mol Å^2) and for reaction coordinates involving angles was 100 kcal/(mol degrees^2).

For all our calculations, the spin-unrestricted approximation was used, and in each case two spin states were taken into consideration.

Results and Discussion

Oxygen Binding Energies. Oxygen affinities were calculated using eq 1, for both oxidation states and also in presence and absence of the substrate. Reaction energy profiles for oxygen binding were not computed, since the barriers associated with the process are usually small[55] and would not be relevant for understanding the PHM mechanism. The oxygenated PHM resting state, $Cu_B^{II}–O_2^{\bullet-}$, was evaluated in both the singlet and triplet spin states, and it was found that the triplet state is more stable, with and without bound substrate. Without the coordinated oxygen, the spin ground state was determined to be the singlet. Evaluation of the oxygenated state, after ET to Cu_B, $Cu_B^{I}–O_2^{\bullet-}$, in both the doublet and quartet spin states indicated that the doublet is the ground state in all cases. The calculated oxygen binding energies of the states are shown in Table 1, together with the high-spin/low-spin energy gaps (ΔE_{HS-LS}) and the relevant Mulliken charge and spin populations (*e*). Relevant numbering of atoms in the QM subsystem used in all calculations is shown in Figure 1.

Table 2 shows some relevant geometrical parameters of all species involved in the calculation of the oxygen affinities. From the two tables, it can be concluded that molecular oxygen binds to Cu_B^{I}, resulting in a species that can be described as $Cu_B^{II}–O_2^{\bullet-}$. The substrate does not appear to make any significant

(43) Warshel, A.; Levitt, M. *J. Mol. Biol.* **1976**, *103*, 227−249.
(44) Zhang, X.; Harrison, D. H. T.; Cui, Q. *J. Am. Chem. Soc.* **2002**, *124*, 14871−14878.
(45) Ryde, U. *Curr. Op. Chem. Biol.* **2003**, *7*, 136−142.
(46) Ridder, L.; Harvey, J. N.; Rietjens, I. M. C. M.; Vervoort, J.; Mulholland, A. J. *J. Phys. Chem. B* **2003**, *107*, 2118−2426.
(47) Schöneboom, J. C.; Cohen, S.; Lin, H.; Shaik, S.; Thiel, W. *J. Am. Chem. Soc.* **2004**, *126*, 4017−4034.
(48) Devi-Kesavan, L. S.; Gao, J. *J. Am. Chem. Soc.* **2003**, *125*, 1532−1540.
(49) Crespo, A.; Scherlis, D. A.; Martí, M. A.; Ordejón, P.; Roitberg, A. E.; Estrin, D. A. *J. Phys. Chem. B* **2003**, *107*, 13728−13736.
(50) Soler, J. M.; Artacho, E.; Gale, J.; García, A.; Junquera, J. Ordejón, P.; Sánchez-Portal, D. J. *Phys: Cond. Matt.* **2002**, *14*, 2745−2779.
(51) Troullier, N.; Martins, J. L. *Phys. Rev. B* **1991**, *43*, 1993−2006.
(52) Louie, S. G.; Froyen, S.; Cohen, M. L. *Phys. Rev. B* **1982**, *26*, 1738−1742.
(53) Perdew, J. P.; Burke, K.; Ernzerhof, M. *Phys. Rev. Lett.* **1996**, *77*, 3865−3868.
(54) Eichinger, M.; Tavan, P.; Hutter, J.; Parrinello, M. *J. Chem. Phys.* **1999**, *110*, 10452−10467.
(55) Franzen, S. *Proc. Natl. Acad. Sci. U.S.A.* **2002**, *99*, 16754−16759.

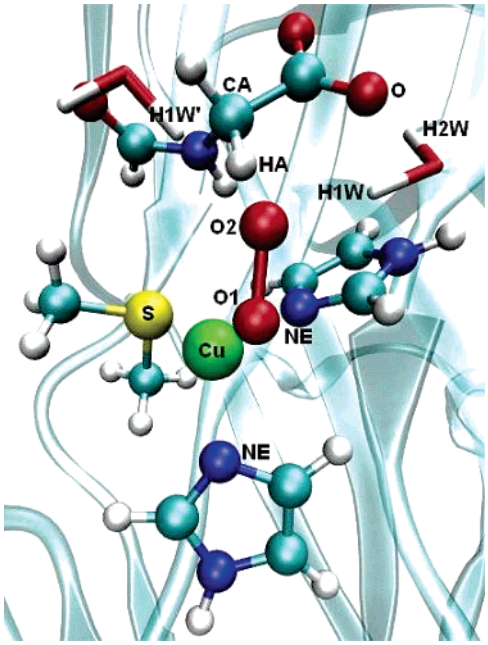

Figure 1. Relevant numbering of the QM subsystem employed in all calculations.

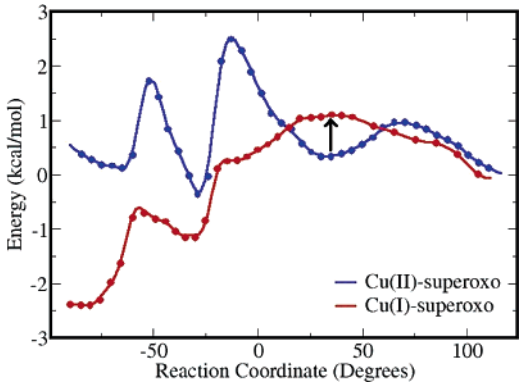

Figure 2. Potential energy profile (kcal/mol) along the $S_{Met314}-Cu-O1-O2$ dihedral angle (degrees) in the $Cu_B^{II}-O_2^{\bullet-}$ (blue) and $Cu_B^{I}-O_2^{\bullet-}$ (red) species. The arrow shows the differences in energy between the two forms when the O_2 is at the orientation found in the crystallographic structure.

difference, as the value of the oxygen binding energy is about − 20 kcal/mol in both cases. However, once oxygen is coordinated, ET to form the $Cu_B^{I}-O_2^{\bullet-}$ species is more favored because the oxygen has a much higher binding energy, about − 69 kcal/mol in the presence of substrate compared to −53 kcal/mol without substrate. The higher oxygen affinity of $Cu_B^{I}-O_2^{\bullet-}$ compared to that of $Cu_B^{II}-O_2^{\bullet-}$ can be attributed to the higher degree of π-back-donation in the former species, which strengthens the bond. This effect is stronger when the metal is in a low oxidation state because more electron density is available. This is the case for the $Cu_B^{I}-O_2^{\bullet-}$ species, in which this effect is reflected in a longer O1−O2 bond (1.31 Å and 1.40 Å in $Cu_B^{II}-O_2^{\bullet-}$ and $Cu_B^{I}-O_2^{\bullet-}$, respectively) and in an increase of the negative Mulliken population of the coordinated O_2 (−0.404*e* and −0.885*e* in $Cu_B^{II}-O_2^{\bullet-}$ and $Cu_B^{I}-O_2^{\bullet-}$, respectively) due to the larger population of the O_2 π^* anti-ligand orbital. Moreover, the substrate considerably increases the binding energy in $Cu_B^{I}-O_2^{\bullet-}$, suggesting that O_2 is more prone to coordination once the substrate is already bound in the enzyme active site, as reported by Prigge et al.[34] The structural basis of this increase in binding energy can be understood using the data from Table 2. With substrate present, there is a strong H-bond interaction between the O2 atom and the surrounding waters (O2−H1W distance of 1.63 Å and 1.81 Å with and without substrate, respectively). Moreover, this water molecule, which has been suggested to be involved in the ET pathway, has a close contact with the substrate carboxylate ($H2W-O_{subs}$ distance of 1.66 Å). This makes the water position more constrained, producing an increase in the O_2 binding energy when the substrate is present. The O2 atom strongly interacts with the substrate *pro-S* HA (O2−HA distance of 2.20 Å and HA atom Mulliken charge of −0.176*e*), further stabilizing the coordinated O_2 in presence of the substrate. This information suggests that once the O_2 binds to PHM, ET is favored, forming the $Cu_B^{I}-O_2^{\bullet-}$, the species with the highest binding energy, and that O_2 binds more favorably to the reduced enzyme after substrate binding.

Oxygen Rotational Motion. To assess the role of the molecular motion involved in the PHM reaction and following the conclusions presented by Prigge et al.[34] we calculated the potential energy profile along the $S_{Met314}-Cu-O1-O2$ dihedral angle (ξ_{O2}) in both $Cu_B^{II}-O_2^{\bullet-}$ (blue curve) and $Cu_B^{I}-O_2^{\bullet-}$ (red curve) species in the presence of substrate (Figure 2). The $Cu_B^{II}-O_2^{\bullet-}$ crystallographic angle of 40° corresponds to a local minimum along the energy surface.[34] The surface has two other minima corresponding to dihedral angles of −30° and −65°. This last corresponds to the rotation of about 110° proposed by Prigge et al.[34] (see also Table 2). Moreover, the rotation of the O_2 along this surface reaches a lower-energy minimum, in which

Table 2. Relevant Geometrical Parameters of All Species Involved in the Calculation of the Oxygen Affinities (Distances in Å, Angles and Dihedrals in deg)

	$Cu_B^{II}-O_2^{\bullet-}$				$Cu_B^{I}-O_2^{\bullet-}$			
	with substrate		without substrate		with substrate		without substrate	
	oxy	free	oxy	free	oxy	free	oxy	free
O1−O2	1.31	−	1.30	−	1.40	−	1.38	−
Cu−O1	1.99	−	2.01	−	1.97	−	1.96	−
$Cu-S_{Met314}$	2.33	2.27	2.33	2.30	2.29	2.25	2.31	2.30
$Cu-N\epsilon_{His242}$	2.04	1.99	2.04	1.99	2.17	1.93	2.12	1.95
$Cu-N\epsilon_{His244}$	1.99	1.94	1.98	1.93	2.07	1.96	2.03	1.97
O2−HA	2.41	−	−	−	2.20	−	−	−
O2−H1W	1.84	−	2.04	−	1.63	−	1.81	−
O2−H1W′	2.05	−	2.14	−	1.77	-	1.75	−
$H2W-O_{subs}$	1.64	1.62	-	−	1.66	1.69	-	−
Cu−O1−O2	120. 8	−	119.4	−	118.0	−	123. 8	−
$S_{Met314}-Cu-O1-O2$	−65.0	−	−58.1	−	−29.5	−	−93. 3	−

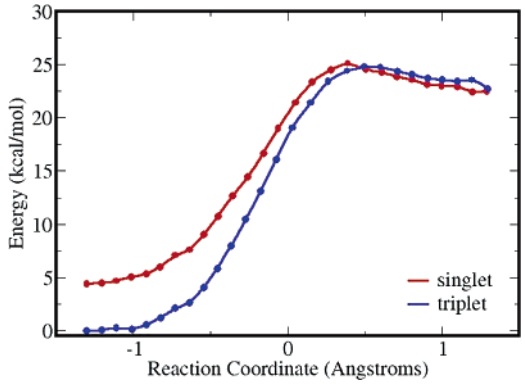

Figure 3. Potential energy profile (kcal/mol) for HA-abstraction reaction catalyzed by $Cu_B^{II}-O_2^{\bullet-}$, reaction (2), in both singlet (red) and triplet (blue) spin surfaces. The reaction coordinate is −1.3 Å in reactants ($Cu_B^{II}-O_2^{\bullet-}$ + HA − CA − subs) and 1.3 Å in products ($[Cu_B^{II}-OOHA]^+$ + CA−subs).

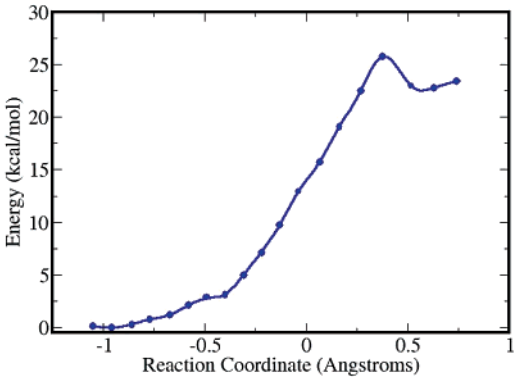

Figure 4. Potential energy profile (kcal/mol) for HA-abstraction reaction catalyzed by $Cu_B^{I}-O_2^{\bullet-}$, reaction (3), in the doublet spin surface. The reaction coordinate is −1.0 Å in the reactants ($Cu_B^{I}-O_2^{\bullet-}$ + HA − CA − subs) and 0.7 Å in the product s ($Cu_B^{I}-OOHA$] + CA − subs).

the O2 atom points toward the substrate *pro-S* HA atom with distance less than 2.4 Å. This conformation can be achieved thermally as suggested by Prigge et al.[34] because the energy barrier is only about 2 kcal/mol. Furthermore, in the surface corresponding to the $Cu_B^{I}-O_2^{\bullet-}$ species the reaction coordinate shows the presence of two minima at −30° and −85°, separated by a thermally accessible rotational barrier of about 1 kcal/mol. However, the stable crystallographic angle of 40° is not an energy minimum on this surface.

These results are compatible with two possible mechanisms of electron transfer. In one, ET takes place with O_2 at the crystallographic position ($\xi_{O2} \approx 40°$). Since this position is not an energy minimum for the $Cu_B^{I}-O_2^{\bullet-}$ species, this conformation would spontaneously relax to one of its minima ($\xi_{O2} \approx -30°$), where the O2 atom is positioned directly toward the substrate *pro-S* HA at a distance of about 2.2 Å (see Table 2). In the other, the O_2 would spend a small fraction of the time in the $Cu_B^{II}-O_2^{\bullet-}$ conformation with $\xi_{O2} \approx -30°$. In this conformation the distance between the HA and the oxygen is the shortest, favoring ET. After ET, the $Cu_B^{I}-O_2^{\bullet-}$ formed would be stabilized by the addition of the electron and become trapped in the optimal position for H-abstraction. In either surface, the O2−HA distance corresponding to a reaction coordinate minimum is less than 2.4 Å.

Hydrogen Abstraction Mechanism. This section deals with the identification of the most reactive oxygenated species active in PHM, focusing on how this species is formed. This analysis was carried out to shed light on the molecular basis of the H-abstraction mechanism.

First, we consider H-abstraction by coordinated O_2 in both $Cu_B^{II}-O_2^{\bullet-}$ and $Cu_B^{I}-O_2^{\bullet-}$ species. The H-abstraction by $Cu_B^{II}-O_2^{\bullet-}$ can be represented by the following reaction:

$$Cu_B^{II}-O_2^{\bullet-} + HA - CA - subs \rightarrow [Cu_B^{II}-OOHA]^+ + CA-subs \quad (2)$$

We calculated the energy profile along the reaction coordinate defined as $\xi = d_{CA-HA} - d_{O2-HA}$ in both the singlet and triplet spin states. As can be seen in Figure 3, the ground-state reactant is $Cu_B^{II}-O_2^{\bullet-}$ in the triplet state (∼5 kcal/mol more stable, see Table 1), whereas the product has almost the same energy in both spin states and a change in the spin surface occurs upon reaction. The activation parameters are 25 and 20 kcal/mol for the triplet (blue curve, Figure 3) and singlet states (red curve, Figure 3), respectively. These values are higher than those obtained by Chen and Solomon[28] (14 kcal/mol) or Kamachi et al.[30] (17 kcal/mol) for isolated model systems. It appears that inclusion of the whole protein, as in our calculations, imposes position constraints on the reactants that result in a higher activation energy. These results indicate that this is probably not the mechanism of H-abstraction because the computed activation energy for this reaction is very high compared to the experimental value of $\Delta H^{\ddagger}$ for the C−H cleavage step in PHM of ∼13 kcal/mol obtained by Francisco et al.[13]

The H-abstraction catalyzed by $Cu_B^{I}-O_2^{\bullet-}$ can be described by a similar reaction:

$$Cu_B^{I}-O_2^{\bullet-} + HA - CA - subs \rightarrow [Cu_B^{II}-OOHA] + CA-subs \quad (3)$$

The doublet and quartet spin energy profiles were calculated as a function of the same reaction coordinate, $\xi = d_{CA-HA} - d_{O2-HA}$. However, as the energy of the doublet is 80 kcal/mol lower than that of the quartet (see Table 1) and both surfaces are similar in shape, we only show the results for the doublet surface in Figure 4. The activation energy is this case is of about 25 kcal/mol in both spin states. Although $Cu_B^{I}-O_2^{\bullet-}$ was proposed by Prigge et al.[34] to be the active species responsible for HA-abstraction in PHM, the high activation energy value obtained in this calculation, ∼25 kcal/mol, suggests that $Cu_B^{I}-O_2^{\bullet-}$ is not the active H-abstracting oxygenated species either.

Thus, it appears that a new oxygenated species carries out the H-abstraction. Chen and Solomon[28] and Kamachi et al.[30] proposed that the abstracting species is the copper−hydroperoxo, $[Cu_B^{II}-OOH]^+$, formed upon protonation by a water molecule of the $Cu_B^{I}-O_2^{\bullet-}$. However, the high activation energy calculated for H-abstraction by this species (∼40 kcal/mol) argues against this mechanism. We evaluated both the formation of the $[Cu_B^{II}-OOH]^+$ species and the further H-abstraction reaction. The first reaction can be summarized as follows:

$$Cu_B^{I}-O_2^{\bullet-} + H_3O^+ \rightarrow [Cu_B^{II}-OOH_W]^+ + H_2O \quad (4)$$

To perform this calculation, we added five O_2-coordinating water molecules (Cu_B solvation waters present in whole MD simulations) and a proton to the QM subsystem. The reaction coordinate is defined as $\xi = d_{O2-HW} - d_{HW-OW}$. The reaction

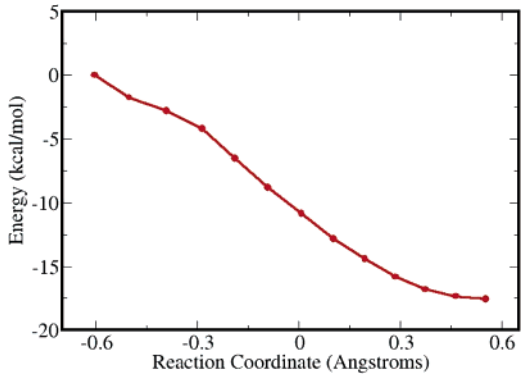

Figure 5. Potential energy profile (kcal/mol) for proton attack by $Cu_B^{I}-O_2^{\bullet-}$ to form $[Cu_B^{II}-OOH]^+$, reaction 4, in the doublet spin state. The reaction coordinate is −0.6 Å in the reactants ($Cu_B^{I}-O_2^{\bullet-} + H_3O^+$) and 0.55 Å in the products ($[Cu_B^{II}-OOH_W]^+ + H_2O$).

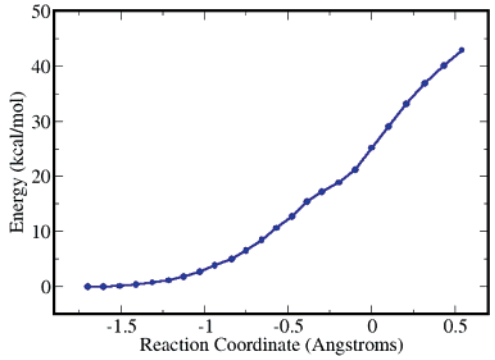

Figure 6. Potential energy profile (kcal/mol) for HA-abstraction reaction catalyzed by $[Cu_B^{II}-OOH]^+$, reaction 5, in the doublet spin state. The reaction coordinate is −1.7 Å in the reactants ($[Cu_B^{II}-O-(OH_WHA)]^+ +$ HA − CA − subs) and 0.55 Å in the products ($[Cu_B^{II}-O-(OH_WHA)]^+ +$ CA−subs).

energy profile was calculated only for the doublet spin state, because the energy of the quartet is 14.5 kcal/mol higher. As can be seen in Figure 5 the reaction occurs spontaneously with no activation energy and with an energy difference of −17.5 kcal/mol, indicating that the $Cu_B^{I}-O_2^{\bullet-}$ species may abstract a proton from the surrounding solvent to form $[Cu_B^{II}-OOH]^+$.

The substrate H-abstraction reaction catalyzed by $[Cu_B^{II}-OOH]^+$ can be written as:

$$[Cu_B^{II}-OOH_W]^+ + HA - CA - subs \rightarrow [Cu_B^{II}-O-(OH_WHA)]^+ + CA-subs \quad (5)$$

The QM subsystem was the same as that used for the previous reaction with the reaction coordinate defined as $\xi = d_{CA-HA} - d_{O2-HA}$. We calculated the reaction energy profile only for the doublet spin state. The corresponding energy profile (blue curve, Figure 6) shows that the $[Cu_B^{II}-OOH]^+$ species cannot abstract the hydrogen from the substrate because the activation energy for this reaction is 42.8 kcal/mol (this value compares well with the 40 kcal/mol obtained by Chen and Solomon[28] and Kamachi et al.[30]).

The question remains how the reaction can proceed if the $[Cu_B^{II}-OOH]^+$ species is formed. On the basis of the reaction stoichiometry, in which two protons are consumed and a water molecule is produced, it is possible for the $[Cu_B^{II}-OOH]^+$ molecule formed to abstract a second proton from the surrounding solvent. By adding another proton to $[Cu_B^{II}-OOH]^+$ and

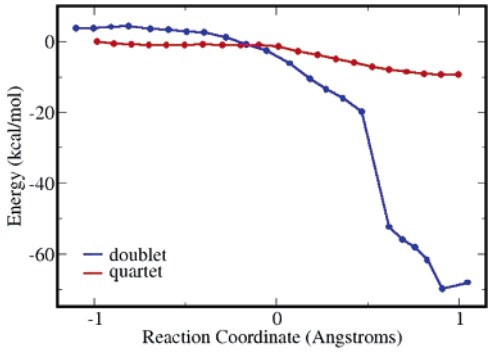

Figure 7. Potential energy profile (kcal/mol) for HA-abstraction reaction catalyzed by $[Cu_BO]^{+2}$ in the quartet spin state (red), reaction 6, with a reaction coordinate value of −1.0 Å in reactants ($[Cu_BO]^{+2}$ + HA − CA − subs) and 0.9 Å in products ($[Cu_BOHA]^{+2}$ + CA − subs), and in the doublet spin state (blue), reaction 7, with a reaction coordinate value of −1.1 Å in reactants ($[Cu_BO]^{+2}$ + HA − CA − subs) and 1.0 Å in products ($[Cu_B]^{+2}$ + HA−O−CA−subs).

optimizing the resulting structure, the following species is obtained, $[Cu_BO\cdots HOH]^{+2}$. The new water molecule coordinated to O1 (HW−O2−HW′) spontaneously twists and coordinates to the O1 atom by one of its hydrogen atoms. The optimized Cu−O1 and O1−HW distances are 1.80 and 2.21 Å, respectively. This result suggests that, once the $Cu_B^{I}-O_2^{\bullet-}$ is formed, it may spontaneously abstract one proton to yield $[Cu_B^{II}-OOH]^+$ and subsequently may abstract another proton to produce the $[Cu_BO]^{+2}$ species with the release of a water molecule. Next, it is necessary to determine whether this copper-monooxygenated species can abstract the hydrogen from the substrate. Taking into account the calculations of Kamachi et al.[30] which showed that $[Cu_BO]^+$ was responsible for H-abstraction in DβM, we calculated the potential energy profiles for H-abstraction catalyzed by either $[Cu_BO]^{+2}$ or $[Cu_BO]^+$ species, in order to test both possibilities for the active oxygenated H-abstracting species in PHM.

The H-abstraction catalyzed by $[Cu_BO]^{+2}$ can be written as follows:

$$[Cu_BO]^{+2} + HA - CA - subs \rightarrow [Cu_BOHA]^{+2} + CA-subs \quad (6)$$

Using the reaction coordinate $\xi = d_{CA-HA} - d_{O1-HA}$, we calculated the reaction energy profile for both the doublet and quartet spin states (Figure 7). The quartet spin state is the ground state of the reactants and is stabilized by 3.8 kcal/mol with respect to the doublet state. The quartet state (red curve, Figure 7) shows an intermediate state in which the abstracted hydrogen forms an OH coordinated to the metal (distances Cu−O1 and O1−HA of 1.86 and 1.00 Å, respectively). The activation energy is negligible (0.15 kcal/mol), and the energy of the intermediate state is 9.4 kcal/mol lower than that of the reactant. The optimized reactive species $[Cu_BO]^{+2}$ accommodates the O1 atom in such a way as to facilitate the abstraction of the HA, as can be seen by the short O1−HA optimized distance of 2.10 Å. The second half of the hydroxylation reaction, the OH binding to the Cα (rebinding step), will be considered later.

The energy profile of the doublet spin state of $[Cu_BO]^{+2}$ (blue curve, Figure 7) is quite different and surprising. In fact, the resulting product is the overall reaction product, the hydroxylated substrate. The activation energy is also negligible (0.16

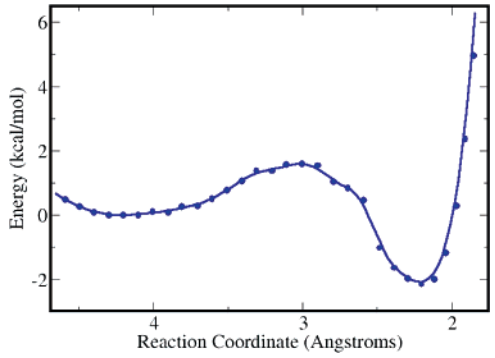

Figure 8. Potential energy profile (kcal/mol) for water coordination to Cu_B^{II}, eq 8. The reaction coordinate varies from 4.6 Å in reactants ($[Cu_B]^{+2}$ + H_2O) to 2.2 Å in products ($[Cu_B\cdots OH_2]^{+2}$).

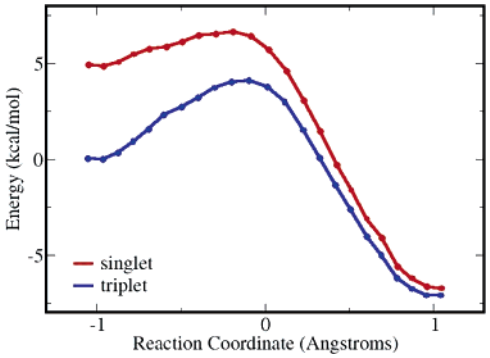

Figure 9. Potential energy profile (kcal/mol) for HA-abstraction reaction catalyzed by $[Cu_BO]^+$ in both singlet (red) and triplet (blue) spin surfaces, corresponding to reaction 9. The reaction coordinate varies from −1.05 Å in reactants ($[Cu_B]^+$ + HA − CA − subs) to 1.05 Å in products ($[Cu_BOHA]^+$ + CA−subs) in both cases.

kcal/mol), and the overall energy difference is −69.9 kcal/mol. This product is ∼60 kcal/mol more stable than the previous intermediate formed on the quartet surface and ∼83 kcal/mol more stable than the corresponding hydroxylated product in the quartet spin state. The spontaneous hydroxylation of the substrate is reflected in the short O1−CA bond distance value (1.43 Å) for the product structure. Thus, the correct reaction on the doublet surface must be considered as:

$$[Cu_BO]^{+2} + HA - CA - subs \rightarrow [Cu_B]^{+2} + HA{-}O{-}CA{-}subs \quad (7)$$

Thus, the reaction pathway involves a spin-inversion electronic process near a crossing region between the quartet and doublet potential energy surfaces. The stable $[Cu_BO]^{+2}$ quartet state must change to the doublet upon H-abstraction, in order to form the hydroxylated product.

To complete the reaction, a water molecule coordinates to $[Cu_B]^{+2}$ to yield $[Cu_B{-}OH_2]^{+2}$, to satisfy the tetrahedral coordination typical of Cu^{II} complexes:

$$[Cu_B]^{+2} + H_2O \rightarrow [Cu_B\cdots OH_2]^{+2} \quad (8)$$

Inspection of the final optimized structure indicates that there are two water molecules (shown in Figure 1) close to the Cu atom with distances from about 4.6 to 5.7 Å. In order to complete the reaction, we have computed the potential energy profile for water coordination to $[Cu_B]^{+2}$ (Figure 8). The chosen reaction coordinate was the shortening of the Cu−OW distance. The energetics of this reaction shows that water coordination is thermodynamically favored by 2.2 kcal/mol with a low-energy barrier of 1.6 kcal/mol. Finally, the $[Cu_B{-}OH_2]^{+2}$ species formed should be reduced by ascorbate to yield $[Cu_B{-}OH_2]^+$ and start the next catalytic cycle upon product release.

As mentioned before, another formal possibility is that the H-abstraction is catalyzed by $[Cu_BO]^+$ obtained after ascorbate reduction. $[Cu_BO]^+$ was proposed to be the abstracting species by Kamachi et al.[30] The H-abstraction catalyzed by $[Cu_BO]^+$ reaction is:

$$[Cu_BO]^+ + HA - CA - subs \rightarrow [Cu_BOHA]^+ + CA{-}subs \quad (9)$$

Using the reaction coordinate $\xi = d_{CA-HA} - d_{O1-HA}$, we calculated the energy profile for both the singlet (red curve, Figure 9) and triplet spin states (blue curve, Figure 9). As can be seen, the triplet spin state is the ground state of the reactants, stabilized by 4.9 kcal/mol with respect to the singlet state, which is almost the same value found by Kamachi et al.[30] (6.5 kcal/mol). The energy profile in the stable triplet state shows the formation of an intermediate in which the abstracted hydrogen forms an OH coordinated to the metal (distances Cu−O1 and O1−HA of 1.89 and 0.99 Å, respectively), with activation energy of 4.1 kcal/mol and an energy difference of −7.1 kcal/mol. These values compare reasonably well with the ones obtained by Kamachi et al.[30] (activation energy 3.8 kcal/mol and energy difference −20 kcal/mol). The energy profile for the excited singlet spin state is similar to that of the triplet, but the activation energy is reduced to 1.8 kcal/mol and the energy of the intermediate formed is only 0.3 kcal/mol higher than that of the triplet.

OH Binding to Cα (Rebinding Step). Energy calculations for the OH rebinding step are necessary to complete the cycle of catalysis by PHM and to decide whether the $[Cu_BO]^+$ is also an active oxygenated species in cases in which the OH-coordinated intermediate is formed, namely $[Cu_BO]^+$ in both the singlet and triplet spin states and $[Cu_BO]^{+2}$ in the quartet spin state. The rebinding reaction can be summarized as follows:

$$[Cu_BOHA]^{+/+2} + CA{-}subs \rightarrow [Cu_B]^{+/+2} + HA{-}O{-}CA{-}subs \quad (10)$$

In all cases the reaction coordinate was $\xi = d_{CA-O1}$ (Figure 10). For OH rebinding from the $[Cu_BOHA]^{+2}$ species in the quartet spin state (green curve, Figure 10), the energy difference is 37.8 kcal/mol, suggesting that this reaction is not thermodynamically spontaneous. This fact is in agreement with those of the calculations described above that suggest a spin-inversion electronic process between the quartet and doublet surfaces and that the hydroxylated product is 83 kcal/mol destabilized in the quartet state. The results of the calculations for the rebinding reaction with the $[Cu_BOHA]^+$ species show that the triplet reactant is only 0.3 kcal/mol more stable. However, the activation energy in the triplet surface is 37.3 kcal/mol (blue curve, Figure 10), whereas it is only 5.4 kcal/mol in the singlet state (red curve, Figure 10). These results suggest that in order to form the hydroxylated product, there must also be a spin-inversion electronic process between the triplet and singlet potential energy surfaces, in agreement with the results obtained by Kamachi et al.[30] (51.4 and 6.5 kcal/mol for the triplet and

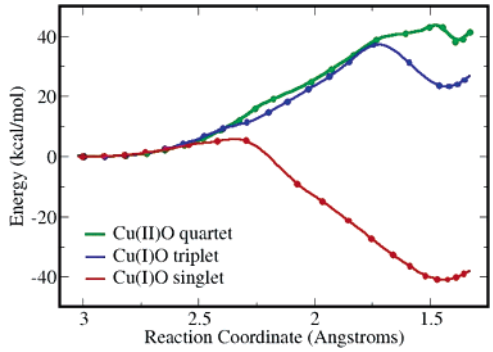

Figure 10. Potential energy profile (kcal/mol) for the rebinding reaction catalyzed by $[Cu_BO]^+$ in both singlet (red) and triplet (blue) spin surfaces and by $[Cu_BO]^{+2}$ in the quartet spin surface (green), corresponding to reaction 10. In all cases, the reaction coordinate varies from 3.0 Å in reactants $(Cu_BOHA]^{+/+2}$ + CA−subs) to 1.4 Å in products ($[Cu_B]^{+/+2}$ + HA−O−CA−subs).

Table 3. Selected Geometrical and Electronic Parameters of $[Cu_BO]^{+2}$ and $[Cu_BO]^+$ Species (Distance in Å, Group Mulliken Charges and Spin Populations (in parenthesis) in *e*)

	$[Cu_BO]^{+2}$		$[Cu_BO]^+$	
spin state	quartet[a]	doublet	triplet[a]	singlet
Cu−O (Å)	1.79	1.80	1.80	1.80
Cu	0.63 (0.62)	0.63 (0.43)	0.62 (0.57)	0.62 (−0.04)
O	−0.41 (1.19)	−0.44 (1.13)	−0.54 (1.06)	−0.57 (0.23)
Met_{314}	0.56 (0.39)	0.53 (0.0)	0.38 (0.20)	0.40 (−0.24)
His_{242}	0.60 (0.28)	0.71 (−0.38)	0.35 (0.07)	0.38 (−0.03)
His_{244}	0.31 (0.12)	0.30 (0.10)	0.23 (0.08)	0.19 (0.06)
L_3	1.47 (0.79)	1.53 (−0.29)	0.96 (0.35)	0.97 (−0.21)
substrate	−0.69 (0.40)	−0.72 (−0.28)	−1.03 (0.03)	−1.02 (0.01)

[a] Ground states.

singlet surfaces, respectively and presence of a spin-inversion process). The energy difference to form the hydroxylated product in the singlet surface is −40.9 kcal/mol. These results suggest that for the rebinding step using the $[Cu_BO]^+$ species only the singlet state is mechanistically feasible. Again, a neighboring water molecule (located at 4.5 to 5.6 Å from Cu) coordinates, and $[Cu_B{-}OH_2]^+$ starts the next catalytic cycle upon product release.

Active Species. The preceding results suggest that both monooxygenated species $[Cu_BO]^{+2}$ and $[Cu_BO]^+$ are able to promote H-abstraction from the substrate. Whereas $[Cu_BO]^{+2}$ abstracts the HA atom concertedly with almost no activation energy and involves a spin-inversion electronic process between the quartet and the doublet states, $[Cu_BO]^+$ forms a OH-coordinated intermediate which continues the reaction with a rebinding step also involving a spin-inversion between the triplet and the singlet states. The active species more likely to be responsible for the H-abstraction in PHM is $[Cu_BO]^{+2}$, because it can abstract the substrate HA atom with almost zero activation energy, yielding the hydroxylated product. Geometrical and electronic parameters for both species are reported in Table 3.

From the results in Table 3, it can be seen that the Cu_BO moiety is equivalent in both species and can be interpreted as $[Cu_B^{III}O]^+$ or $[Cu_B^{II}{-}O^{\bullet-}]^+$, since Cu−O distances are very similar (∼1.8 Å), and the Mulliken charges and spin populations are almost the same. The difference between both species resides mainly in the electronic properties of the ligand residues coordinated to Cu: in the $[Cu_BO]^{+2}$ species there is significant positive charge and unpaired electron density localized over the three ligands coordinated to Cu_B, which can be thought of as $L_3^{+\bullet}$, whereas in $[Cu_BO]^+$ the ligands carry less positive charge and almost no unpaired electron density. This fact suggests that in the reduced $[Cu_BO]^+$ species, the extra electron is located mainly on the ligands. The $[Cu_BO]^{+2}$ species can then be assigned as $[L_3^{\bullet+}Cu_B^{III}O]^{+2}$ or $[L_3^{\bullet+}Cu_B^{II}O^{\bullet-}]^{+2}$, consisting in a triplet $[Cu_B^{III}O]^+/[Cu_B^{II}{-}O^{\bullet-}]^+$ moiety ferromagneticaly and antiferromagneticly coupled with $L_3^{\bullet+}$ in the quartet and doublet states, respectively. On the other hand, the reduced $[Cu_BO]^+$ species can be assigned as $[L_3Cu_B^{III}O]^+$ or to $[L_3Cu_B^{II}O^{\bullet-}]^+$ with a two-unpaired-electrons $[Cu_B^{III}O]^+/[Cu_B^{II}{-}O^{\bullet-}]^+$ moiety, in the ground triplet spin state. These results are in agreement with those reported by Kamachi et al. for the $[Cu_BO]^+$ species.[30]

An important finding is that both $[L_3^{\bullet+}Cu_B^{III}O]^{+2}$ and $[L_3Cu_B^{III}O]^+$ species resemble their iron analogues, Compounds I ($Por^{\bullet+}Fe^{IV}O$, Por = porphyrin) and II ($PorFe^{IV}O$), respectively.[56] These intermediates have been detected for various peroxidases and are believed to be involved in the reaction mechanism of cytochromes P450 enzymes.[57−59] In the consensus rebound mechanism for aliphatic H-abstractions performed by cytochromes P450 enzymes suggested by Groves et al.,[57,59−63] the active species is Compound I. Several theoretical studies were focused on this H-abstraction reaction together with the characterization of both Compounds I and II.[56,64−66] The Fe−O distances, Mulliken charges, and spin populations over the FeO moiety have been reported to be almost the same for Compounds I and II (two unpaired electrons), but in the former species a third unpaired electron is located on a porphyrin orbital in the quartet state.[56] The Mulliken charge and spin populations over the oxygen atom in Compound I, computed by Shaik's and Yoshinawa's groups,[64,66] are similar to the values obtained for the $[Cu_BO]^{+2}$ species. The overall mechanism in cytochrome P450 involves O_2 coordination, one-electron reduction, two-proton consumption (and one water molecule release) to form Compound I, the species responsible for H-abstraction and substrate hydroxylation.[64−66] Our computational results indicate that the probable active species in PHM is $[L_3^{\bullet+}Cu_B^{III}O]^{+2}$, which resembles its iron analogue active species in P450 (Compound I), suggesting that both PHM and cytochrome P450 enzymes may carry out substrate hydroxylation by using a similar mechanism.

Finally, it is interesting to note that in PHM the catalytic center, Cu_B, is solvent exposed, as reported in the crystallographic structure and also confirmed by our MD simulations, suggesting that the two protons responsible for formation of $[L_3^{\bullet+}Cu_B^{III}O]^{+2}$ may arise from the surrounding water molecules. Then, simultaneous availability of two solvent protons on the distal oxygen is a requirement for PHM enzymatic efficacy. The involvement of solvent in protonation reactions is a common paradigm in heme-enzyme catalysis.[67] Moreover,

(56) Ghosh, A.; Almlöf, J.; Que, L., Jr. *J. Phys. Chem.* **1994**, *98*, 5576−5579.
(57) Groves, J. T.; Han, Y.-Z. In *Cytochrome P450: Structure, Mechanism and Biochemistry*, 2nd ed.; Ortiz de Montellano, P. R., Ed.; *Plenum Press: New York*, **1995**; p 3.
(58) Sono, M.; Roach, M. P.; Coulter, E. D.; Dawson, J. H. *Chem. Rev.* **1996**, *96*, 2841.
(59) Groves, J. T. *J. Chem. Educ.* **1985**, *62*, 928.
(60) Groves, J. T.; McClusky, G. A. *J. Am. Chem. Soc.* **1976**, *98*, 859.
(61) Groves, J. T.; van der Puy, M. *J. Am. Chem. Soc.* **1976**, *98*, 5290.
(62) Groves, J. T.; Subramanian, D. V. *J. Am. Chem. Soc.* **1984**, *106*, 2177.
(63) Groves, J. T.; Watanabe, Y. *J. Am. Chem. Soc.* **1988**, *110*, 8443.
(64) Schöneboom, L. H.; Reuter, N.; Thiel, W.; Cohen, S.; Ogliaro, F.; Shaik, S. *J. Am. Chem. Soc.* **2002**, *124*, 8142−8151.
(65) Guallar, V.; Friesner, R. A. *J. Am. Chem. Soc.* **2004**, *126*, 8501.
(66) Kamachi, T.; Yoshizawa, K. *J. Am. Chem. Soc.* **2003**, *125*, 4652.
(67) Harris, D. L.; Loew, G. H. *J. Am. Chem. Soc.* **1998**, *120*, 8941−8948.

Scheme 6. Proposed Mechanism Operative in PHM[a]

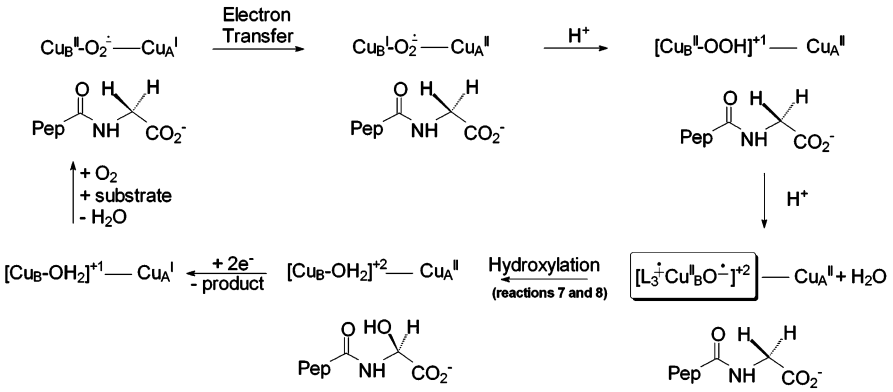

[a] The $[L_3^{\bullet+}Cu_B^{II}O^{\bullet-}]^{+2}/[L_3^{\bullet+}Cu_B^{III}O]^{+2}$ species resembles cytochrome P450 active species Compound I, and is believed to be responsible for H-abstraction in PHM.

after substrate hydroxylation, the reaction is completed when a water molecule binds to the fourth coordination position of $[Cu_B]^{+2}$ and ascorbate reduces $[Cu_B{-}OH_2]^{+2}$ to $[Cu_B{-}OH_2]^{+}$, starting another catalytic cycle upon product release. The overall mechanism suggested by the preceding results is schematically shown in Scheme 6. Nevertheless, the crucial question of how the long-range ET between the Cu_A and Cu_B sites occurs also needs further elaboration.

Conclusions

This work reports the results of QM-MM calculations aimed at studying the mechanism of catalysis by PHM. The reaction consists of the hydroxylation of the C of a glycine residue at the C-terminal position of a glycine-extended peptide or protein. Calculations of O_2 binding energy to Cu^I_B suggest that molecular oxygen binds to the copper, resulting in the $Cu_B^{II}{-}O_2^{\bullet-}$ species. The $Cu_B^{I}{-}O_2^{\bullet-}$ species may be formed by subsequent ET. Stabilization of this species results because the coordinated oxygen has a much higher binding energy in this case due to a greater π-back-donation effect. Moreover, the substrate considerably increases the binding energy of $Cu_B^{I}{-}O_2^{\bullet-}$ due to closer interactions and geometric constraints, suggesting that O_2 is more prone to coordination once the substrate is already in place in the enzymatic active site. These results are in agreement with the rotational barrier calculation of the distal oxygen atom around the $Cu_B{-}O$ bond. Once the O_2 binds, leading to a $Cu_B^{II}{-}O_2^{\bullet-}$ minimum conformation of 40°, ET occurs to form the $Cu_B^{I}{-}O_2^{\bullet-}$ species but in an energy maximum conformation, which can subsequently relax to one of its minima, where the oxygen atom is located directly toward the substrate *pro-S* HA.

Calculations were also used to identify the most reactive oxygenated species active in PHM, paying particular attention to how this species was formed. Potential energy profiles computed for the H-abstraction reaction for both $Cu_B^{II}{-}O_2^{\bullet-}$ and $Cu_B^{I}{-}O_2^{\bullet-}$ species suggest that due to their high activation energies none of them is responsible for the abstraction. Inspection of the potential energy surfaces shows that the $[Cu_B^{II}{-}OOH]^{+}$ species is spontaneously formed by abstracting a proton from the surrounding solvent, but cannot abstract the hydrogen atom from the substrate. However, this species can spontaneously abstract another proton from the surrounding solvent to form $[L_3^{\bullet+}Cu_B^{III}O]^{+2}$ (a two-unpaired-electrons $[Cu_B^{III}O]^{+}$ moiety ferromagneticaly coupled with $L_3^{\bullet+}$, in the quartet spin ground state) with a water molecule released. Finally, we evaluated whether this monooxygenated species or the one obtained by prior reduction with ascorbate, $[L_3Cu_B^{III}O]^{+}$, was able to promote H-abstraction from the substrate. The calculations show that both species are able to produce H-abstraction. $[L_3^{\bullet+}Cu_B^{III}O]^{+2}$ abstracts the HA atom concertedly with almost no activation energy and involving a spin-inversion electronic process from the quartet reactant ground state to the doublet product ground-state potential energy surfaces. However, $[L_3Cu_B^{III}O]^{+}$ abstracts the hydrogen to form an intermediate with OH coordinated in the triplet surface with an activation energy of 4.1 kcal/mol. Moreover, this intermediate continues the reaction with a rebinding step that has an activation energy of 5.4 kcal/mol. This process also involves a spin-inversion from the triplet reactant ground state to the singlet product ground-state potential energy surfaces.

The results of these calculations suggest that the active species responsible for the H-abstraction by PHM obtained in this work is probably $[L_3^{\bullet+}Cu_B^{III}O]^{+2}$, which resembles its iron analogue active species in cytochrome P450 enzymes (Compound I), also suggesting that both enzymes may carry out substrate hydroxylation by using a similar mechanism, as shown in Scheme 6. This suggestion is consistent with the existing experimental information[32,35] and with the lower overall activation energy. Moreover, this active species is formed exothermically by abstracting two protons from the surrounding solvent and can abstract the substrate HA atom without activation energy to form the hydroxylated product via a mechanism similar to that of the cytochrome P450 enzymes (Scheme 6).[64−66] Finally, a neighboring water molecule binds to Cu_B to complete the tetrahedral coordination of this copper. Upon release of the hydroxylated peptide product, ascorbate reduces $[Cu_B{-}OH_2]^{+2}$ to $[Cu_B{-}OH_2]^{+}$, starting another catalytic cycle. Insights regarding the catalytic mechanism of PHM obtained in this work may apply to other copper−oxygen-activating enzymes, such as DβM, and may aid to the design of biomimetic copper complexes.

Acknowledgment. This work was partially supported by grants from Fundación Antorchas, Universidad de Buenos Aires, and ANPCYT (PICT 06-08447) and a NSF Grant (MCB-

0450465) to LMA. Computer resources were provided by the Large Allocations Resource Committee through Grant TG-MCA05S010 to A.E.R. A.C. acknowledges Antti Puisto for providing the copper pseudopotential and basis for Siesta.

Supporting Information Available: This material is available free of charge via the Internet at http://pubs.acs.org.

JA062876X